Intercalation of a Multiply Bonded Dimolybdenum Core into Layered Metal Phosphates

Yeung-gyo K. Shin and Daniel G. Nocera*,†

Contribution from the Department of Chemistry and the Center for Fundamental Materials Research, Michigan State University, East Lansing, Michigan 48824. *Received July 22, 1991. Revised Manuscript Received September 23, 1991*

Abstract: The spectroscopic and magnetic properties of a quadruply bonded dimolybdenum core intercalated into the layered metal phosphates (LMPs) of vanadium and niobium have been examined. Layer modification of the LMPs was achieved by redox intercalation of the Mo_2^{4+} core solvated by acetonitrile and by its ion-exchange reaction following reduction of the phosphate host layers with $NaBH_4$. Regardless of the reaction pathway, a similar product is obtained. The reacted layers display a contraction of the d-spacing with concomitant insertion of up to 0.2 molybdenum atoms per layer unit cell. Structural characterization and absorption spectroscopy of these materials reveal that the bimetallic core residing in the gallery interlayer region is the mixed-valence Mo_2^{5+} center in a transverse orientation. In this arrangement the ubiquitous D_{4h} coordination environment of multiply bonded "Mo_2O_8" complexes is achieved with the dimolybdenum core keyed into tetragonal oxygen cavities of the layer. Magnetic susceptibility and EPR studies reveal that electrons in the layers are antiferromagnetically coupled and that the exchange interaction is in a weak coupling regime. This exchange interaction is enhanced by the presence of the paramagnetic Mo_2^{5+} center within the interlayer region of the LMP.

Introduction

A common design of many light-to-energy conversion photochemical schemes is predicated on the electron transfer chemistry of the photosynthetic reaction center. In photosynthesis, photon absorption by the light harvesting complex promotes efficient transmembrane electron/hole separation of the pair, which is ultimately manifested in the multielectron chemistry of water oxidation at the oxygen-evolving complex and proton reduction in Photosystem I.[1-12] Accordingly, the design of biomimetic assemblies has relied on the synthesis of charge separating networks that propagate efficient electron/hole separation on different time scales. The basic tenet of the approach involves the transport of charge separated electrons and holes away from a light harvesting center by covalently attaching donors and acceptors to it. Perhaps the most straightforward donor/acceptor system, in both concept and structure, are coordination compounds possessing a lowest energy excited state that involves the promotion of an electron from a metal-based orbital to a ligand-based orbital.[13-17] Ensuing recombination of the ligand-centered electron and metal-centered hole can be slow, which is a prerequisite for efficient charge separation. The donor/acceptor strategy has been further elaborated with the development of porphyrin-based diads[18-27] and triads.[27-30] In the former, porphyrins covalently juxtaposed to other porphyrin or quinone acceptors in cofacial and edge-on geometries yield charge separated states upon excitation of the porphyrin. Introduction of an electron donor onto the porphyrin photoreceptor in Gust and Moore's[28] and Wasielewski's[29] triads permits the photogenerated hole localized on the porphyrin to be trapped by the following sequence of charge separating electron transfer events: $DP^*A \rightarrow DP^+A^- \rightarrow D^+PA^-$. Although this photogenerated charge separated state may persist into the microsecond range, the quantum yield can be relatively low.[31]

In an effort to achieve better charge separation, the covalently bonded molecular approach to vectorial charge separation has been complemented by the vectorial arrangement of electron transfer components within organized architectures. Systems designed about many support structures, such as micelles,[32-36] polymers,[37] and solid state substrates,[38-44] have been investigated. For example, one particularly intriguing approach is that of Mallouk et al.,[45] who have catenated a metalloporphyrin or $Ru(bpy)_3^{2+}$ photosensitizer to a methylviologen charge transfer/Pt catalyst self-assembly organized within the channels of Zeolite-L. The microstructure of the zeolite causes a spatially organized triad (sacrificial electron donor, photosensitizer, electron transfer carrier) to form at the zeolite/solution interface.

† Alfred P. Sloan Fellow and NSF Presidential Young Investigator.

(1) (a) Babcock, G. T.; Barry, B. A.; Debus, R. J.; Hoganson, C. W.; Atamian, M.; McIntosh, L.; Sithole, I.; Yocum, C. F. *J. Am. Chem. Soc.* **1989**, *28*, 9557. (b) Babcock, G. T. In *New Comprehensive Biochemistry: Photosynthesis*; Amesz, J., Ed.; Elsevier: Amsterdam, 1987.
(2) Allen, J. P.; Feher, G.; Yeates, T. O.; Rees, D. C.; Deisenhofer, J.; Michel, H.; Huber, R. *Proc. Natl. Acad. Sci. U.S.A.* **1986**, *83*, 8589.
(3) Gunner, M. R.; Dutton, P. L. *J. Am. Chem. Soc.* **1989**, *111*, 3400.
(4) (a) Manchanda, R.; Thorp, H. H.; Brudvig, G. W.; Crabtree, R. H. *Inorg. Chem.* **1991**, *30*, 494. (b) Sarneski, J. E.; Thorp, H. H.; Brudvig, G. W.; Crabtree, R. H.; Schulte, G. K. *J. Am. Chem. Soc.* **1990**, *112*, 7255. (c) Brudvig, G. W.; Crabtree, R. H. *Prog. Inorg. Chem.* **1989**, *37*, 99.
(5) Christou, G. *Acc. Chem. Res.* **1989**, *22*, 328.
(6) Wieghardt, K. *Angew. Chem., Int. Ed. Engl.* **1989**, *28*, 1153.
(7) Friesner, R. A.; Won, Y. *Biochim. Biophys. Acta, Rev. Bioenerg.* **1989**, *99*, 977.
(8) (a) McDowell, L. M.; Kirmaier, C.; Holten, D. *J. Phys. Chem.* **1991**, *95*, 3379. (b) Kirmaier, C.; Holten, D. In *The Photosynthetic Bacterial Reaction Center—Structure and Dynamics*; Breton, J., Vermeglio, A., Eds.; Plenum: New York, 1988; p 219.
(9) Chan, M. K.; Armstrong, W. H. *J. Am. Chem. Soc.* **1990**, *112*, 4985.
(10) Renger, G. *Angew. Chem., Int. Ed. Engl.* **1987**, *26*, 643. (b) Renger, G. In *Biophysics*; Hoppe, W., Lohmann, W., Markl, H., Ziegler, H., Eds.; Springer-Verlag: Berlin, 1983; Chapter 13, p 515.
(11) Johnson, S. G.; Tang, D.; Jankowiak, R.; Hayes, J. M.; Small, G. J. *J. Phys. Chem.* **1990**, *94*, 5849.
(12) Fox, M. A. *Photochem. Photobiol.* **1990**, *52*, 617.
(13) (a) Duesing, R.; Tapolsky, G.; Meyer, T. J. *J. Am. Chem. Soc.* **1990**, *112*, 5378. (b) Chen, P.; Duesing, R.; Tapolsky, G.; Meyer, T. J. *J. Am. Chem. Soc.* **1989**, *111*, 8305. (c) Meyer, T. J. *Acc. Chem. Res.* **1989**, *22*, 164.
(14) Perkins, T. A.; Humer, W.; Netzel, T. L.; Schanze, K. S. *J. Phys. Chem.* **1990**, *94*, 2229.
(15) Winslow, L. N.; Rillema, D. P.; Welch, J. H.; Singh, P. *Inorg. Chem.* **1989**, *28*, 1596.
(16) *Photoinduced Electron Transfer*; Mattay, J., Ed.; Springer-Verlag: New York, 1990; Vol. II.
(17) Vogler, A.; Kunkely, H. *Comm. Inorg. Chem.* **1990**, *9*, 210.
(18) (a) Helms, A.; Heiler, D.; McLendon, G. *J. Am. Chem. Soc.* **1991**, *113*, 4325. (b) Heiler, D.; McLendon, G.; Rogalskij, P. *J. Am. Chem. Soc.* **1987**, *109*, 604.
(19) Antolovich, M.; Keyte, P. J.; Oliver, A. M.; Paddon-Row, M. N.; Kroon, J.; Verhoeven, J. W.; Jonker, S. A.; Warman, J. M. *J. Phys. Chem.* **1991**, *95*, 1933.
(20) Batova, E. E.; Levin, P. O.; Shafirovich, V. Y. *New J. Chem.* **1991**, *14*, 269.
(21) Osuka, A.; Maruyama, K.; Mataga, N.; Asahi, T.; Yamazaki, I.; Tamai, N. *J. Am. Chem. Soc.* **1990**, *112*, 4958.
(22) (a) Gaines, G. L., III; O'Neil, M. P.; Svec, W. A.; Niemczyk, M. P.; Wasielewski, M. R. *J. Am. Chem. Soc.* **1991**, *113*, 719. (b) Wasielewski, M. R.; Johnson, D. G.; Niemczyk, M. P.; Gaines, G. L., III; O'Neil, M. P.; Svec, W. A. *J. Am. Chem. Soc.* **1990**, *112*, 6482. (c) Wasielewski, M. R.; Johnson, D. G.; Svec, W. A.; Kersey, K. M.; Minsek, D. W. *J. Am. Chem. Soc.* **1988**, *110*, 7219. (d) Wasielewski, M. R.; Niemczyk, M. P. *ACS Symp. Ser.* **1986**, *321*, 154.

0002-7863/92/1514-1264$03.00/0

Even with the successful design of charge separating networks, multielectron photochemistry is not ensured. The initial electron/hole pair must be stored at the terminus of the network, and the overall process must be repeated to build up the necessary multielectron hole and electron equivalents. Ultimately, the charge equivalents must then be coupled to a catalytic center capable of promoting the overall multielectron process. The intricacies required to molecularly engineer such elegant charge separating networks containing the capacity for storage and catalytic bookends prompted us to consider a new conceptual direction. If more than one electron can be moved from a discrete excited state, then the structural complexity demanded for efficient charge separation should be relaxed. Moreover, multielectron reaction from an electronically excited core obviates the necessity for charge storage coupled to catalytic redox centers.

To this end, we have become interested in designing solid state assemblies in which a multielectron photoactive center is incorporated between redox active layers of a host structure. In principle, regeneration of the oxidized photoactive core can be achieved with auxiliary redox-active metal centers in the solid state support; subsequent reaction of substrate at the layers will reestablish the formal oxidation state of metals in supporting solid state substrates thereby completing the catalytic cycle. In this approach, relay molecules are not required since the multielectron chemistry does not rely on the charge propagation via one-electron intermediates of a charge separation network. The exclusion of the relay system leads to an important advantage of this approach in that the intricate structural engineering of photoactive solids needed to prevent charge recombination is circumvented. Our recent discovery of two-electron photoreactions of quadruply bonded metal–metal ($M\overset{4}{-}M$) systems[46] has prompted us to begin designing structures in which $M\overset{4}{-}M$ cores are incorporated into layered host structures containing redox-active metal centers in the layers. Of course the design of such a structure requires physical and chemical compatibility between supporting host structures and $M\overset{4}{-}M$ bimetallic complexes. Our early studies concentrated on complex layered oxides (CLOs) as layered supports.[47] But we soon realized early in our studies that the utilization of CLOs is hindered by the following crucial factors: (i) the metals composing the layers of CLO structures are generally redox-inactive[48-50] and difficult to substitute;[51] (ii) the basicity of CLOs is not compatible with the properties of many transition metal complexes and especially the $M\overset{4}{-}M$ species, which are susceptible to the formation of hydroxo and oxo complexes;[52] and (iii) the chemical properties of CLOs, for the most part, are too irreproducible for reliable photochemical study. Conversely, layered metal phosphates (LMPs) are superb host compounds for binuclear metal cores because they are acidic and may be synthesized to yield pure crystalline materials featuring redox-active metals composing the layered host structure.[53-58] In addition LMPs display high stability toward temperature, irradiation, and most organic environments.

We now report the synthetic methodologies for the incorporation of a multiply bonded dimolybdenum core within layered vanadium and niobium phosphates. Our choice for the the synthesis of a LMP intercalated with a bimetallic molybdenum core was motivated by our extensive knowledge of the structure, spectroscopy, and chemistry of the quadruply bonded Mo_2(II,II), mixed-valence Mo_2(II,III), and triply bonded Mo_2(III,III) cores coordinated by

(23) (a) Schmidt, J. A.; McIntosh, A. R.; Weedon, A. C.; Bolton, J. R.; Connolly, J. S.; Hurley, J. K.; Wasielewski, M. R. *J. Am. Chem. Soc.* **1988**, *110*, 1733. (b) Siemiarczuk, A.; McIntosh, A. R.; Ho, T.-F.; Stillman, M. J.; Roach, K. J.; Weedon, A. C.; Bolton, J. R.; Connolly, J. S. *J. Am. Chem. Soc.* **1983**, *105*, 7224.

(24) (a) Mataga, N.; Yao, H.; Okada, T.; Kanda, Y.; Harriman, A. *Chem. Phys.* **1989**, *131*, 473. (b) Sakata, Y.; Nakashima, S.; Goto, Y.; Tatemitsu, H.; Misumi, S.; Asahi, T.; Hagihara, M.; Nishikawa, S.; Okada, T.; Mataga, N. *J. Am. Chem. Soc.* **1989**, *111*, 8979.

(25) (a) Bilsel, O.; Rodriguez, J.; Holten, D. *J. Am. Chem. Soc.* **1990**, *112*, 4075. (b) Knapp, S.; Dhar, T. G. M.; Albaneze, J.; Gentemann, S.; Potenza, J. A.; Holten, D.; Schugar, H. J. *J. Am. Chem. Soc.* **1991**, *113*, 4010.

(26) (a) Harrison, R. J.; Pearce, B.; Beddard, G. S.; Cowan, J. A.; Sanders, J. K. M. *Chem. Phys.* **1987**, *116*, 429. (b) Hunter, C. A.; Meah, M. N.; Sanders, J. K. M. *J. Am. Chem. Soc.* **1990**, *112*, 5773.

(27) Leland, B. A.; Jordan, A. D.; Felker, P. M.; Hopfield, J. J.; Zewail, A.; Dervan, P. B. *J. Phys. Chem.* **1985**, *89*, 5571.

(28) (a) Gust, D.; Moore, T. A.; Moore, A. L.; Gao, F.; Luttrull, D.; DeGraziano, J. M.; Ma, X. C.; Making, L. R.; Lee, S.-J.; Trier, T. T.; Bittersmann, E.; Seely, G. R.; Woodward, S.; Bensasson, R. V.; Rougee, M.; De Schryver, F. C.; Van der Auweraer, M. *J. Am. Chem. Soc.* **1991**, *113*, 3638. (b) Hasharoni, K.; Levanon, H.; Tang, J.; Bowman, M. K.; Norice, J. R.; Gust, D.; Moore, T. A.; Moore, A. L. *J. Am. Chem. Soc.* **1990**, *112*, 6477. (c) Gust, D.; Moore, T. A.; Moore, A. L.; Lee, S.-J.; Bittersmann, E.; Luttrull, D. K.; Rehms, A. A.; DeGraziano, J. M.; Ma, X. C.; Gao, F.; Belford, R. E.; Trier, T. A. *Science* **1990**, *248*, 199. (d) Gust, D.; Moore, T. A.; Moore, A. L.; Makins, L. R.; Seely, G. R.; Ma, X.; Trier, T. T.; Gao, F. *J. Am. Chem. Soc.* **1988**, *110*, 7567. (e) Gust, D.; Moore, T. A. In *Supramolecular Photochemistry*; Balzani, V., Ed.; Reidel: Boston, 1987.

(29) (a) Wasielewski, M. R.; Gaines, G. L., III; O'Neil, M. P.; Svec, W. A.; Niemczyk, M. P. *J. Am. Chem. Soc.* **1990**, *112*, 4559. (b) Wasielewski, M. R.; Minsek, D. W.; Niemczyk, M. P.; Svec, W. A.; Yang, N. C. *J. Am. Chem. Soc.* **1990**, *112*, 2823. (c) Wasielewski, M. R. In *Photoinduced Electron Transfer*; Fox, M. A., Chanon, M., Eds.; Elsevier: Amsterdam, 1988; Part A, p 161. (d) Wasielewski, M. R.; Niemczyk, M. P.; Svec, W. A.; Pewitt, E. B. *J. Am. Chem. Soc.* **1985**, *107*, 5562.

(30) Rodriguez, J.; Kirmaier, C.; Johnson, M. R.; Friesner, R. A.; Holten, D.; Sessler, J. L. *J. Am. Chem. Soc.* **1991**, *113*, 1652.

(31) Gust, D.; Moore, T. A.; Moore, A. L.; Barrett, D.; Makings, L. R.; Liddell, P. A.; DeSchryver, F. C.; Van der Auweraer, M.; Benssasson, R. V.; Rougee, M. *J. Am. Chem. Soc.* **1988**, *110*, 321.

(32) Yamazaki, I.; Tamai, N.; Yamazaki, T. *J. Phys. Chem.* **1990**, *94*, 516.

(33) Haubs, M.; Kingsdorf, H. *New J. Chem.* **1987**, *11*, 151.

(34) Kunitake, T. *New J. Chem.* **1987**, *11*, 141.

(35) Thomas, J. K. *Chem. Rev.* **1980**, *80*, 283.

(36) Tricot, Y.-M.; Porat, Z.; Manassen, J. *J. Phys. Chem.* **1991**, *95*, 3242.

(37) Krishnan, M.; White, J. M.; Fox, M. A.; Bard, A. J. *J. Am. Chem. Soc.* **1983**, *105*, 7002.

(38) (a) Cervera-March, S.; Smatkin, E. S.; Bard, A. J.; Campion, A.; Fox, M. A.; Mallouk, T. E.; Webber, S. E.; White, J. M. *J. Electrochem. Soc.* **1988**, *135*, 567. (b) Fox, M. A.; Cardona, R.; Gaillard, E. *J. Am. Chem Soc.* **1987**, *109*, 6347. (c) Sobczynski, A.; Bard, A. J.; Campion, F.; Fox, M. A.; Mallouk, T. E.; Webber, S. E.; White, J. M. *J. Phys. Chem.* **1987**, *91*, 3316. (d) Fox, M. A. *New J. Chem.* **1987**, *11*, 129. (e) Pettit, T. L.; Fox, M. A. *J. Phys. Chem.* **1986**, *90*, 1353.

(39) (a) Duonghong, D.; Serpone, N.; Grätzel, M. *Helv. Chim. Acta* **1984**, *67*, 1012. (b) Houlding, V. H.; Grätzel, M. *J. Am. Chem. Soc.* **1983**, *105*, 5696. (c) Humphry-Baker, R.; Lilie, J.; Grätzel, M. *J. Am. Chem. Soc.* **1982**, *104*, 442.

(40) (a) Thomas, J. K. *Acc. Chem. Res.* **1988**, *21*, 275. (b) Thomas, J. K.; Hashimoto, S. *New J. Chem.* **1987**, *11*, 145.

(41) Pichat, P. *New J. Chem.* **1987**, *11*, 135.

(42) Nijs, H.; Fripiat, J. J.; Damme, H. V. *J. Phys. Chem.* **1983**, *87*, 1279.

(43) Tsubomura, H.; Nakato, Y. *New J. Chem.* **1987**, *11*, 167.

(44) Yoon, K. B.; Kochi, J. K. *J. Phys. Chem.* **1991**, *95*, 3780.

(45) (a) Krueger, J. S.; Mayer, J. E.; Mallouk, T. E. *J. Am. Chem. Soc.* **1988**, *110*, 8232. (b) Persaud, L.; Bard, A. J.; Campion, A.; Fox, M. A.; Mallouk, T. E.; Webber, S. E.; White, J. M. *J. Am. Chem. Soc.* **1987**, *109*, 7309.

(46) (a) Partigianoni, C. P.; Turro, C.; Shin, Y.-g. K.; Motry, D. H.; Kadis, J.; Dulebohn, J. I.; Nocera, D. G. *Mixed Valency Systems: Applications in Chemistry, Physics, and Biology*; Kluwer Academic: Dordrecht, 1991; p 91. (b) Partigianoni, C. P.; Chang, I-J.; Nocera, D. G. *Coord. Chem. Rev.* **1990**, *97*, 105. (c) Partigianoni, C. P.; Nocera, D. G. *Inorg. Chem.* **1990**, *29*, 2033.

(47) Newsham, M. D.; Giannelis, E. P.; Pinnavaia, T. J.; Nocera, D. G. *J. Am. Chem. Soc.* **1988**, *110*, 3885.

(48) King, R. D.; Nocera, D. G.; Pinnavaia, T. J. *J. Electroanal. Chem.* **1987**, *236*, 43.

(49) (a) Ege, D.; Ghosh, P. K.; White, J. R.; Equey, J.-F.; Bard, A. J. *J. Am. Chem. Soc.* **1985**, *107*, 5644. (b) Ghosh, P. K.; Bard, A. J. *J. Am. Chem. Soc.* **1983**, *105*, 5691.

(50) Liu, H. Y.; Anson, F. C. *J. Electroanal. Chem.* **1985**, *184*, 411.

(51) Whittingham, M. S.; Jacobson, A. J. *Intercalation Chemistry*; Academic Press: New York, 1982.

(52) Dulebohn, J. I.; Ward, D. L.; Nocera, D. G. *Polyhedron* **1991**, in press.

(53) (a) Clearfield, A.; Thakur, D. S. *Appl. Catal.* **1986**, *26*, 1. (b) Clearfield, A. In *Inorganic Ion-Exchange Materials*; Clearfield, A., Ed.; CRC Press: Boca Raton, FL, 1982.

(54) Casan, N.; Amoros, P.; Ibanez, R.; Tamoyo, E. M.; Beltran-Porter, A.; Beltran-Porter, D. *J. Inclusion Phenom.* **1988**, *6*, 195.

(55) Garcia-Ponce, A. L.; Moreno-Real, L.; Limenez-Lopez, A. *Inorg. Chem.* **1988**, *27*, 3372.

(56) Chahboun, H.; Groult, D.; Hervieu, M.; Raveau, B. *J. Solid State Chem.* **1986**, *65*, 331.

(57) Stranford, G. T.; Condrate, R. A., Sr. *J. Solid State Chem.* **1984**, *52*, 248.

(58) (a) Bordes, E.; Courtine, P. *J. Chem. Soc., Chem. Commun.* **1985**, 294. (b) Bordes, E.; Courtine, P. *J. Catal.* **1979**, *57*, 236.

phosphate ion.[59-61] The coordination sphere of the dimolybdenum core in the resulting solid is analogous to these molecular bimetallic phosphates, and redox intercalation chemistry of the Mo_2–LMP system affords materials with interesting magnetic properties.

Experimental Section

Synthesis. Solvents used for syntheses were dried by refluxing over the proper drying agent under nitrogen atmosphere for at least 24 h. Starting materials were purchased from either Aldrich Chemical or Strem Chemical Co. and used as received.

The fully solvated dimolybdenum core in acetonitrile was obtained by the esterification of acetate ligands of $Mo_2(CH_3COO)_4$,[62] which was synthesized by the standard methods.[63,64] A suspension of bright yellow, crystalline $Mo_2(CH_3COO)_4$ (0.2 g, 0.5 mmol) in deoxygenated CH_3CN (15 mL) was charged with 10 mL of a 1 M CH_2Cl_2 solution of $(CH_3C-H_2)_3OBF_4$ to produce a wine-red solution. The reaction mixture was refluxed under a static head of argon for 3 days. The mixture was cooled in an ice-bath to yield $[Mo_2(CH_3CN)_8](BF_4)_4$, which was filtered under a blanket of argon, washed with three 10-mL portions of CH_2Cl_2, and dried under vacuum. The resulting blue powder was air-sensitive and decomposed within minutes in air; decomposition of the compound was accelerated by the presence of moisture.

Layered vanadium and niobium phosphates were obtained by standard procedures.[65,66] The light brown powder of V_2O_5 (12.6 g, 69 mmol) was added to dilute phosphoric acid (100 mL, 28%, 460 mmol) to ensure a 7:1 ratio of phosphorus to vanadium. Upon refluxing the mixture, a brown to greenish-yellow color change indicated the formation of $VOPO_4{\cdot}2H_2O$. Over 3 days of reflux, shiny yellow-green microcrystals of $VOPO_4{\cdot}2H_2O$ precipitated from the reaction mixture. After filtration, the solid was washed with water and acetone and air-dried. The layered material $NbOPO_4{\cdot}3H_2O$ was synthesized by dissolving metallic niobium (5 g, 54 mmol) in a mixture of HF (50 mL, 40%) and nitric acid (5 mL, concentrated), with subsequent addition of phosphoric acid (30 mL, 85%). Excess HF was removed by heating the clear solution on a water bath until the white solid of $NbOPO_4{\cdot}3H_2O$ appeared at the solution/air interface. The resulting solution was cooled to room temperature and the solid was collected by filtration. The solid was washed by its successive suspension and filtration in nitric acid (300 mL, 5 M), water (200 mL), and ethanol (200 mL). The vanadium and niobium layered phosphates were characterized by X-ray powder diffraction and FTIR.[67-70] It is noteworthy that the powder X-ray diffraction pattern of the latter phosphate showed multiple phases when the solid was washed simply by suction filtration and not subjected to the multiple re-suspension/filtration procedure.

The Na^+-intercalated layers were obtained by reacting neutral layers with $NaBH_4$. This modification of Jacobson's NaI reduction procedure[71] avoids contamination of the solid with I_2. Addition of $VOPO_4{\cdot}2H_2O$ (2 g, 10 mmol) to a $NaBH_4$ (0.4 g, 10 mmol) suspension in dried, deoxygenated THF led $VOPO_4{\cdot}2H_2O$ to become dark-green. The reaction was accompanied by a less than vigorous evolution of hydrogen gas. After 1 h of stirring, the dark-green solid was filtered and washed with THF and several portions of water to remove unreacted $NaBH_4$. The resulting crystalline powder was further washed with acetone and air-dried. The same procedure was used to produce Na^+-intercalated $NbOPO_4$. However, no color change was observed upon the reduction of $NbOPO_4{\cdot}3H_2O$.

The incorporation of solvated dimolybdenum cores into LMPs was achieved by direct intercalation or by ion-exchange of the Na^+-intercalated LMP. Insertion reactions were carried out in dried, deoxygenated acetonitrile owing to the extreme sensitivity of the acetonitrile-solvated Mo_2^{4+} core toward oxidation. In a typical reaction, an acetonitrile solution of $[Mo_2(CH_3CN)_8](BF_4)_4$ (0.4 g, 0.5 mmol, 2 mequiv) was transferred onto the layered material (0.1 g, ~0.5 mmol) under argon and the mixture was stirred 3–7 days after a static head of argon. Unfortunately, the progress of reaction was rather difficult to observe. Therefore the desirable reaction period, usually 3 days, was determined by recording X-ray diffraction patterns of solid extracted from the reaction mixture at 24-h intervals. Upon completion of the reaction, the solid was filtered and washed with acetonitrile and diethyl ether and air-dried. Dimer intercalated LMPs were stored in an Ar filled drybox.

Instrumentation and Methods. Elemental analysis of LMPs was performed with a Perkin-Elmer PHI 4500 ESCA system, which is housed in the Composite Materials and Structure Center at Michigan State University. The X-ray source was the monochromated Al Kα line ($E_{Al(K\alpha)}$ = 1486.6 eV, $P_{Al(K\alpha)}$ = 600 W/15 kV). Samples to be analyzed were pressed onto double-sided tape adhered to a stage, which was placed at a 65° angle to the incident X-ray beam under ultrahigh vacuum (10^{-8}–10^{-9} Torr). The sample stage was positioned so that the signal intensity for oxygen (binding energy of 531 eV) was maximized because oxygen was the most abundant element in the LMPs. Elements were identified by survey scans over the range of binding energies from 1200 to 0 eV. The strongest photoelectron line from each element was scanned separately to obtain relative atomic concentrations by integrating the area of the peak and multiplying an appropriate response factor. Elemental compositions were determined from at least three separate analyses; the standard deviation in all cases was less than 5%. All data manipulations were accomplished on an Apollo Workstation using XPS ESCA software provided by the manufacturer.

Infrared spectra were recorded on a Nicolet 740 FTIR spectrometer. A KBr beam splitter/DTGS-KBr detector was employed for the mid-IR spectral region whereas the Far-IR Solid Substrate beam splitter/DTGS-PE detector was employed for the far-IR spectral range. Solid KBr or CsI pellet samples were prepared, depending on the spectral region, and an average of 16 scans was used for data collection. Absorption spectra, obtained with a Cary 17 spectrophotometer, were measured on KBr pellets.

Powder X-ray diffraction patterns were recorded on a Rotaflex system from Rigaku. The Cu Kα line was obtained from a rotating Cu anode (45 kV, 50 mA) and directed toward the sample chamber by using a 1/2 deg divergence slit and a 1/2 deg receiving slit. The diffracted X-ray beam was further refined by a curved graphite single crystal monochromator (1.05 deg scatter slit and 1/6 deg monochromator receiving slit), which was set for detection of the secondary X-ray diffraction line. The compounds were mounted by pressing dried powder on a piece of double-sided tape of 1 in. × 0.5 in. dimensions adhered to a glass slide. The resulting data were recorded and processed by using the manufacturer-provided software DMAXB on a microVAX computing system.

Electron paramagnetic resonance spectra of LMPs were measured by using a Bruker ER 200D X-band spectrometer equipped with an Oxford ESR-9 liquid helium cryostat. Magnetic fields were measured with a Bruker ER 035M gaussmeter, and the microwave frequency was measured with a Hewlett-Packard 5245L frequency counter. The layered compound was placed into a quartz tube equipped with a Kontes quick release stopcock and evacuated until the pressure was less than 5×10^{-5} Torr. Variation of temperature was achieved by controlling the flow rate of gas generated from a liquid helium reservoir or placing sample tubes in a finger Dewar flask filled with liquid nitrogen. Spectral simulations were performed using PROGRAM POWD developed by Belford et al. at the University of Illinois.[72]

Magnetic susceptibilities were measured on a SHE 800 series variable-temperature SQUID magnetometer controlled by an IBM-PC microcomputer. A known quantity of layered compound was placed in a KEL-F bucket, whose magnetic susceptibility was independently determined for its application as a correction factor to observed sample susceptibilities. Measurements were made with an ascending temperature ramp to 300 K followed by a descending ramp in an effort to observe hysteresis, if there was any. Actual readings were made only after the temperature was observed to be stabilized within ±5%. Typically, ten measurements were averaged for one temperature setting; all readings were within a ±5% error limit.

Results and Discussion

Synthesis of Layered Metal Phosphates. The structure of vanadium and niobium phosphates consists of an array of alternating M^VO_6 octahedra and PO_4 tetrahedra that share their corners.

(59) (a) Chang, I-J.; Nocera, D. G. *Inorg. Chem.* **1989**, *28*, 4309. (b) Chang, I-J.; Nocera, D. G. *J. Am. Chem. Soc.* **1987**, *109*, 4901. (c) Chang, I-J.; Hammermesh, M. A.; Nocera, D. G. Submitted for publication.

(60) (a) Bino, A. *Inorg. Chem.* **1981**, *20*, 623. (b) Bino, A.; Cotton, F. A. *Angew. Chem., Int. Ed. Engl.* **1979**, *18*, 462. (c) Bino, A.; Cotton, F. A. *Inorg. Chem.* **1979**, *18*, 3562.

(61) Hopkins, M. D.; Miskowski, V. M.; Gray, H. B. *J. Am. Chem. Soc.* **1988**, *108*, 959.

(62) Cotton, F. A.; Wiesinger, K. J. *Inorg. Chem.* **1991**, *30*, 871.

(63) Lawton, D.; Mason, R. *J. Am. Chem. Soc.* **1965**, *87*, 921.

(64) Stephenson, T. A.; Banniester, E.; Wilkinson, G. *J. Chem. Soc.* **1964**, 2538.

(65) Ladwig, V. G. *Z. Anorg. Allg. Chem.* **1965**, *338*, 266.

(66) Beneke, K.; Lagaly, G. *Inorg. Chem.* **1983**, *22*, 1503.

(67) R'kha, C.; Vandenborre, M. T.; Livage, J.; Prost, R.; Huard, E. *J. Solid State Chem.* **1986**, *63*, 202.

(68) Johnson, J. W.; Jacobson, A. J.; Brody, J. F.; Rich, S. M. *Inorg. Chem.* **1982**, *21*, 3820.

(69) Bordes, E.; Courtine, P.; Pannetier, G. *Ann. Chim. (Paris)* **1973**, *8*, 105.

(70) Chernoeukov, N. G.; Egorov, N. P.; Mochalova, I. R. *Russ. J. Inorg. Chem.* **1978**, *23*, 1627.

(71) Jacobson, A. J.; Johnson, J. W.; Brody, J. F.; Scanlon, J. C.; Lewandowski, J. T. *Inorg. Chem.* **1985**, *24*, 1782.

(72) Belford, R. L.; Nilges, M. J. *Computer Simulation of Powder Spectra*; EPR Symposium, 21st Rocky Mountain Conference: Denver, CO, 1979.

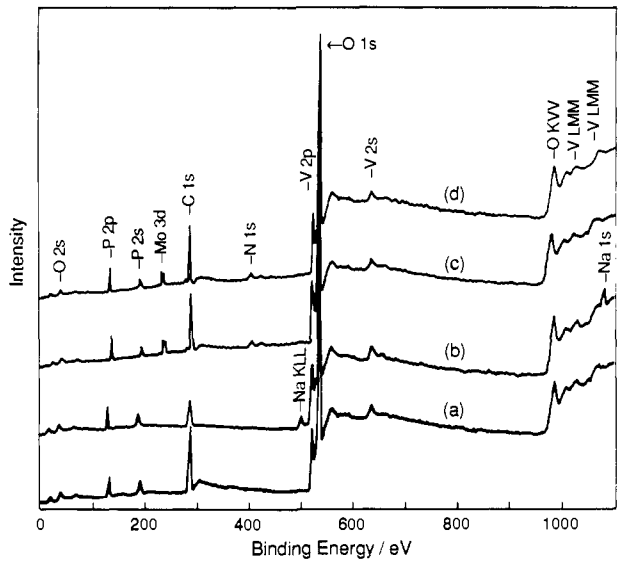

Figure 1. ESCA spectra of (a) $VOPO_4{\cdot}2H_2O$, (b) Na^+-intercalated $VOPO_4$ host layers, and the solids obtained from the reaction of $[Mo_2(CH_3CN)_8](BF_4)_4$ with (c) $VOPO_4{\cdot}2H_2O$ and (d) Na^+-intercalated $VOPO_4$.

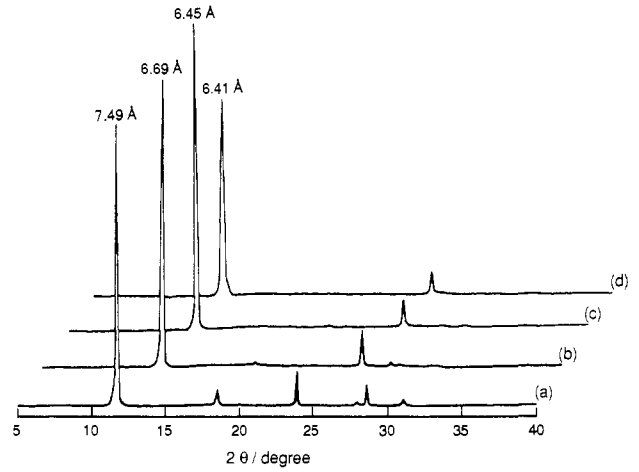

Figure 2. Powder X-ray diffraction patterns of (a) $VOPO_4{\cdot}2H_2O$, (b) Na^+-intercalated $VOPO_4$ host layers, and the solids obtained from the reaction of $[Mo_2(CH_3CN)_8](BF_4)_4$ with (c) $VOPO_4{\cdot}2H_2O$ and (d) Na^+-intercalated $VOPO_4$. All traces cover the same range of 2θ values, but traces b–d are offset for clarity of presentation. The d_{001} peaks are labeled for each spectrum.

Specifically, four equatorial oxygens of the M^VO_6 are provided by four different adjacent phosphate groups. The apical positions of the M^VO_6 octahedron are completed with a terminal M=O bond and a coordinating oxygen from one of two gallery waters. This corner sharing of phosphates to the M^V center is extended in two-dimensions to produce sheets of $[(H_2O)MOPO_4]_n$ that are stacked in the crystallographic *c*-direction.[51,73–75] The second water molecule resides in the gallery between phosphate groups of adjacent layers.

Because the central metal ions are in their highest formal oxidation state M^V, the reduction of these centers is a facile chemical process. In fact, metal centers in the M^{IV} state are one of the most common defects in $VOPO_4$ type layered compounds.[67,73–76] Since the layer does not carry any exchangeable ions, incorporation of compounds into $VOPO_4$ type layers proceeds by redox intercalation whereupon reduction of the layer is accompanied by inclusion of positively charged ions in order that charge neutrality is maintained.[53,71,76]

The introduction of a Mo_2 core into the LMP is most easily accomplished by employing $Mo_2(CH_3CN)_8^{4+}$ as a source. Facile ligand exchange of the solvating acetonitrile is the pre-eminent reaction pathway of this dimer. Oxidation of Mo_2^{4+} cores to mixed-valence Mo_2^{5+} or triply bonded Mo_2^{6+} cores[59] provides the driving force for the redox intercalation chemistry. Alternatively, the high positive charge of the Mo_2^{4+} solvate facilitates its ion-exchange of LMPs intercalated by simple inorganic cations.

To this end, $Mo_2(CH_3CN)_8^{4+}$ was reacted with $VOPO_4{\cdot}2H_2O$ by the two separate routes shown in Schemes I and II. Scheme I represents the redox intercalation pathway, whereas Scheme II is the ion-exchange reaction pathway following reduction of the layers with $NaBH_4$. The distinct steps of the reaction sequence are conveniently monitored by ESCA. Figure 1a is the ESCA survey scan of native $VOPO_4$. Peaks characteristic of V (523, 784, 1017 eV), P (133, 191 eV) and O (531 eV) are prominent. Additionally, the C 1s peak at 289 eV is observed, which is a commonly observed impurity in ESCA spectra.[77] The P/M stoichiometry, obtained by normalizing the P 1p peak areas to those of V 2p photoelectron features, is slightly greater than the expected value of unity (P/V = 1.15).

Scheme I

$$VOPO_4{\cdot}2H_2O \xrightarrow{Mo_2(CH_3CN)_8^{4+}} VOPO_4^{n(x-)}{\cdot}(Mo_2^{n+})_x \quad (1)$$

Scheme II

$$VOPO_4{\cdot}2H_2O \xrightarrow{NaBH_4} VOPO_4^{y-}{\cdot}(Na^+)_y \quad (2)$$

$$VOPO_4^{y-}{\cdot}(Na^+)_y \xrightarrow{Mo_2(CH_3CN)_8^{4+}} VOPO_4^{n(z-)}{\cdot}(Mo_2^{n+})_z \quad (3)$$

Reduction of the host $VOPO_4{\cdot}2H_2O$ by $NaBH_4$ (Scheme II) induces several changes in the ESCA spectrum. Most obviously, as shown in Figure 1b, the Na 1s photoelectron peak at 1072 eV appears. From the peak area we calculate that the Na^+ content of the intercalated $VOPO_4$ is 0.34 thereby yielding a product with a composition of $VOPO_4{\cdot}Na_{0.34}$. The oxygen content, which we define as the number of oxygen atoms per one metal center in the layer, is slightly decreased with intercalation of Na^+ (~7%). This result is in accordance with a reduction in the interlayer spacing of the solid (vide supra), which presumably is accompanied by loss of interlayer water from the more restricted environment. However, small changes in CO_2 impurity concentrations could also account for our observation. The layer stability toward intercalation is in evidence by the fact that the P/M ratio does not change upon introduction of Na^+ into the LMP gallery.

ESCA spectra of the molybdenum intercalate prepared by Scheme II, shown in Figure 1d, reveal that the Na^+ ions undergo complete exchange in the presence of $Mo_2(CH_3CN)_8^{4+}$. The absence of the Na 1s photoelectron peak at 1072 eV is complemented by the appearance of a broad feature at 230 eV attributable to the $3d_{5/2,3/2}$ doublet of molybdenum. The stoichiometry of the solid, as determined by ESCA, is $VOPO_4{\cdot}Mo_{0.19}$. We believe that this observed metal content represents the highest possible loading for these layers because the same loadings are observed even when ion-exchange is performed from solutions containing the guest complex at concentrations ~5 times the redox capacity of host layers. Interestingly, the ESCA survey scan recorded on solids obtained from the direct reaction of $Mo_2(CH_3CN)_8^{4+}$ ion with $VOPO_4{\cdot}2H_2O$ (Figure 1c) is virtually identical to that observed for the ion-exchange pathway, as is the chemical composition of $VOPO_4{\cdot}Mo_{0.17}$.

The X-ray powder diffraction patterns of LMPs produced by Schemes I and II are also similar. Figure 2 displays X-ray diffraction patterns of the $VOPO_4$ host and its intercalates. A d_{001} peak at 7.49 Å (2θ = 11.80°) and higher order peaks of the native

(73) Bruque, S.; Martinez-Lara, M.; Moreno-Real, L.; Jimenez-Lopez, A.; Casal, B.; Ruiz-Hitzky, E. *Inorg. Chem.* **1987**, *26*, 847.
(74) Tachez, M.; Theobald, F.; Bernard, J.; Hewat, A. W. *Rev. Chim. Miner.* **1982**, *19*, 291.
(75) Jordan, B.; Calvo, C. *Can. J. Chem.* **1973**, *51*, 2721.
(76) Yakovleva, T. N.; Tarasova, D. V.; Mikheikin, I. D.; Timoshenko, V. I. *Russ. J. Inorg. Chem.* **1988**, *33*, 134.
(77) Swingle, R. S., Jr.; Riggs, W. M. In *Critical Review in Analytical Chemistry*; CRC Press: Boca Raton, FL, 1975.

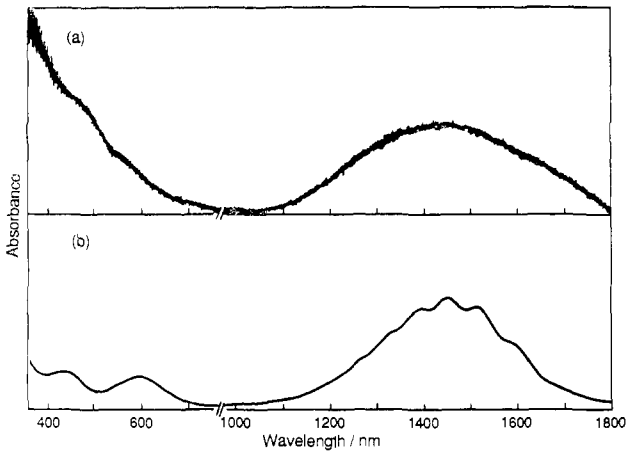

Figure 3. Electronic absorption spectra of (a) $NbOPO_4 \cdot 3H_2O$ reacted with $[Mo_2(CH_3CN)_8](BF_4)_4$ and (b) $Mo_2(HPO_4)_4^{3-}$ in deoxygenated 2 M H_3PO_4.

$VOPO_4 \cdot 2H_2O$ are in excellent agreement with their calculated positions based on published cell parameters (Table I of Supplementary Material).[66-69] Chemical reduction of the layers by $NaBH_4$ causes the d_{001} peak to shift to higher angles indicating a contraction in the layer spacing (d_{001} = 6.69 Å), and a further reduction in the gallery height (d_{001} = 6.41 Å) is observed upon reaction with the $Mo_2(CH_3CN)_8^{4+}$ ion. This gallery height is nearly identical to the 6.45 Å d_{001} spacing of LMP prepared by direct intercalation with $Mo_2(CH_3CN)_8^{4+}$.

Spectroscopy of Layered Metal Phosphates. The nature of the molybdenum species within the LMP prepared by Schemes I and II is revealed by electronic and magnetic spectroscopy.[78] In regard to the former, absorption spectroscopy is particularly useful because the absorption profiles of multiply bonded dimolybdenum cores coordinated by phosphate ions are well established.[59,61] Notwithstanding, the observation of absorption bands from a dimolybdenum guest in a $VOPO_4$ host is problematic because the transitions arising from the reduced V(IV) centers of the layer cause the intercalated solid to absorb throughout the visible spectral region (λ_{max} = 850, 640, 470, and 300 nm)[59b] thereby obscuring the relatively weak absorptions expected from a dimolybdenum phosphate core. By contrast, the isostructural LMP of $NbOPO_4$ does not exhibit transitions in the visible upon its reduction and hence absorption of guest molecules can in principle be spectrally distinguished. Thus the intercalation chemistry described by Schemes I and II was performed for $NbOPO_4 \cdot 3H_2O$.

The ESCA results for layered niobium phosphate materials produced by Schemes I and II are entirely analogous with our observations for the $VOPO_4$ system, with the only major difference of course being the absence of vanadium photoelectron features and the ocurrence of niobium peaks. These data have been included as Supplementary Material. The chemical compositions of solids obtained by Schemes I and II were $NbOPO_4 \cdot Mo_{0.16}$ and $NbOPO_4 \cdot Mo_{0.12}$, respectively. The molybdenum contents of these solids are comparable to that observed for the vanadium system. Moreover, the gallery heights of the intercalates prepared by the independent routes were identical (d_{001} = 7.12 Å for Schemes I and II). Consistent with our observations of the $VOPO_4$ system, these d-spacings are reduced by nearly 1.0 Å from that of the native LMP structure (see Supplementary Material). Thus the intercalation chemistry of the vanadium and niobium LMPs with $Mo_2(CH_3CN)_8^{4+}$ is parallel.

The white layers of $NbOPO_4 \cdot 3H_2O$ (Scheme I) or Na^+-intercalated $NbOPO_4$ (Scheme II) turn blue-grey upon their exposure to $[Mo_2(CH_3CN)_8](BF_4)_4$ solutions. This color change

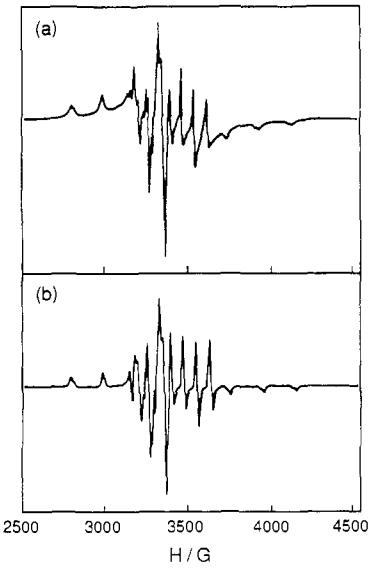

Figure 4. Electron paramagnetic resonance spectra of (a) $VOPO_4 \cdot 2H_2O$ at 7 K and (b) the simulated spectrum calculated by using a two-site model for the d^1 V(IV) centers. The microwave frequency and the sweep range were 9.4711 GHz and 2512–4582 G, respectively.

is noteworthy because the Mo_2(II,II) tetraphosphate is pink whereas the mixed-valence Mo_2(II,III) tetraphosphate is blue-grey.[59b] More quantitatively, Figure 3 shows the electronic absorption spectrum of $NbOPO_4 \cdot Mo_{0.16}$ prepared by Scheme I; an identical spectrum is obtained for $NbOPO_4 \cdot Mo_{0.12}$ prepared by Scheme II. Overlying a rapidly rising baseline, due to scattered light and/or a very broad charge transfer band of the layer itself, two shoulders at ~480 and ~550 nm are observed. This spectrum establishes that the quadruply bonded $Mo_2(HPO_4)_4^{4-}$, which would show an intense $\delta^2 \rightarrow \delta\delta^*$ transition at 516 nm, is not incorporated in the layer. Alternatively, comparison of the absorption spectrum of the mixed-valence $Mo_2(HPO_4)_4^{3-}$ molecular species, which is also shown in Figure 3, clearly establishes the presence of a Mo_2(II,III) core intercalated in $NbOPO_4$. The two weak features in the absorption spectrum of Mo_2-intercalated $NbOPO_4$ are energetically coincident with the $\pi \rightarrow \delta^*$ and $\pi \rightarrow \delta$ transitions of $Mo_2(HPO_4)_4^{3-}$ at 420 and 595 nm, respectively.[61] Even more striking, the characteristic near-IR absorption for the $\delta \rightarrow \delta^*$ transition of the mixed-valence Mo_2(II,III) tetraphosphate centered at 1400 nm is observed for the Mo_2-intercalated $NbOPO_4$ layers. The absence of vibrational fine structure in Figure 3a is most likely due to inhomogeneous line broadening. The similarity of the synthetic conditions for Mo_2-intercalated $NbOPO_4$ and $VOPO_4$ layers suggests to us that this core is retained in the $VOPO_4$ layers.

Magnetic studies are also consistent with intercalation of a Mo_2(II,III) core into LMP. We begin by considering the native $VOPO_4$ layers, whose magnetic susceptibility and EPR spectrum result from the unpaired electrons of V(IV) (d^1) impurity sites.[67,76] The paramagnetism of the solid follows simple Curie–Weiss law behavior, with a linear $1/\chi_M$ vs T plot observed over all temperatures. A free electron spin concentration of 1.8% is calculated from the slope of the Curie–Weiss plot, which suggests a low spin density in the layers arising from isolated V(IV) centers. As expected in an isolated spin system, the low-temperature (8 K) EPR spectrum of the $VOPO_4 \cdot 2H_2O$ layered material, shown in Figure 4a, exhibits a very well defined axial doublet signal, which is consistent with the 4-fold symmetry of the V(IV) center. Figure 4a also shows hyperfine splittings arising from the interaction of the unpaired electron with the nuclear spin of the V(IV) center. Qualitatively, similar EPR signals have been observed from $V^{IV}O^{2+}$ in several different environments, including $V^{IV}O^{2+}$ doped into single crystals of $Rb_2Co(SeO_4)_2 \cdot 6H_2O$,[79] included in Nafion

(78) Attempts to observe the symmetric M–M vibration by IR are prevented because the totally symmetric vibration of multiply bonded dimers is forbidden. Though allowed by Raman spectroscopy, the highly colored $VOPO_4$ (see text) prevents resonance spectra of the symmetric M–M stretch to be obtained owing to sample decomposition.

(79) Jain, V. K. *J. Magn. Reson.* **1985**, *64*, 512.67.

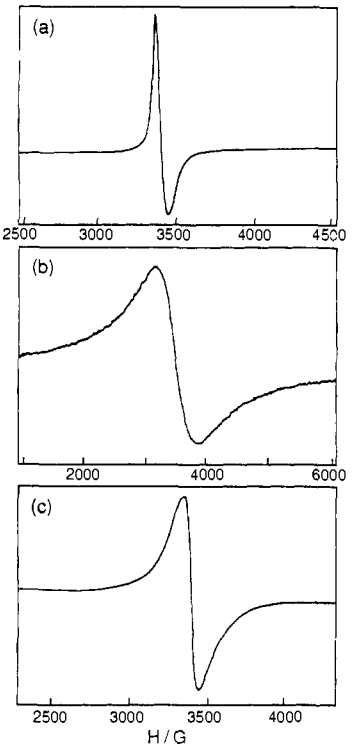

Figure 5. EPR spectra of (a) Na^+-intercalated $VOPO_4$ (9.4724 GHz, 2497–4577 G, $g = 1.96$), (b) Mo_2^{5+}-intercalated $VOPO_4$ (9.4726 GHz, 970–6068 G, $g = 1.95$), and (c) the Mo_2^{5+}-intercalated $VOPO_4$ layers after exposure to air (9.4718 GHz, 2293–4387 G, $g = 1.96$).

membranes,[80] and coordinated to a porphyrin ring.[81] Close inspection of the EPR spectrum reveals two features on the $g_\parallel$ component. As shown in Figure 4b, the observed EPR signal can be simulated by overlapping two simple axial spectra, one with $g_\perp = 1.977$ and $g_\parallel = 1.937$ and the other with $g_\perp = 1.973$ and $g_\parallel = 1.940$. As is the case for Jain's system,[79] a straightforward 8-line spectrum is obtained for a unique d^1 structure. The simulation establishes that the d^1 electrons of the $VOPO_4$ host layer are isolated and occupy two distinct but very closely related vanadium environments. These results are in accordance with the defect model proposed by Bordes et al.,[82] who have shown in their structural study of α-$VOPO_4$ the presence of cis and trans conformations of $V(=O)O_4$ square pyramids about the equatorial V–O–P–O–V chain.

Intercalation of the $VOPO_4$ layers by Na^+ ion causes a significant reduction of V(V) sites to V(IV), and not unexpectedly a change in the magnetism of the LMP is observed. One obvious difference is the complete disappearance of the hyperfine splitting in the EPR spectrum (Figure 5a). The EPR signal displays a Dysonian shape, which is characteristic of conducting electrons exhibiting metallic character.[83] Moreover, the passage effect of saturation at very low power is observed, which is characteristic of Dysonian signals.[83,84] The observation of a Dysonian line shape indicates that the electron density from the d^1 spin centers in the reduced layer is not only high but also interacting over the extended structure.

Partial spin delocalization within the reduced layers is supported by the marked deviation of the magnetic susceptibility from Curie–Weiss behavior at temperatures <20 K. The precipitous drop of $\chi_M T$ with decreasing temperature (Figure 6) reveals an

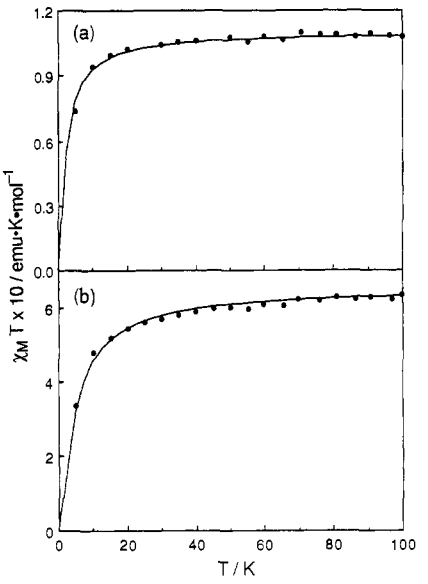

Figure 6. The temperature dependent magnetic susceptibility plots of (a) Na^+-intercalated and (b) Mo_2^{5+}-intercalated $VOPO_4$ layers. The solid lines represent the best fit of eq 4 to the observed data.

antiferromagnetic ordering of the d^1 paramagnetic centers. The sign and strength of the exchange interactions in the vanadyl phosphate intercalate suggest two-dimensional coupling of the d^1 electrons by a superexchange mechanism via phosphate tetrahedra within the *a,b*-plane.[85] As discussed by Rushbrooke[86] and Lines,[87] the magnetic susceptibility for an exchange interaction confined to two-dimensional space is given by a high-temperature expansion series derived for a quadratic layer Heisenberg antiferromagnet

$$\chi_M = \frac{N\langle g\rangle^2\beta^2}{4kT}\left(1 + \frac{2}{\zeta} + \frac{2}{\zeta^2} + \frac{4}{3\zeta^3} + \ldots\right)^{-1} \qquad (4)$$

where $\zeta = kT/J = 2T/\theta$, and N, β, and k are Avogadro's number, the Bohr magneton, and the Boltzmann constant, respectively. An iterative fit of the $\chi_M T$ vs T plot by eq 4 is shown with the solid line in Figure 6a. The excellent correspondence between calculated and experimental data reveals that a weakly coupled antiferromagnetic d^1 center in a two-dimensional plane is a good description for the observed magnetism of the Na^+ intercalate. Moreover the calculated exchange coupling constant of $J/k = -0.88$ K is consistent with the Weiss temperature of θ ($=2J/k$) $= -1.75$ K (as determined from a $1/\chi_M$ vs T plot). This exchange constant accords well with the study of Villeneuve et al. of the isostructural $VOSO_4$ system.[88] In this layered compound, the exchange interaction of d^1 V(IV) centers composing the layers is also weak and antiferromagnetic ($J/k = -0.9$ K).

The magnetic properties of this two-dimensional magnetic system are greatly perturbed upon intercalation of Mo_2(II,III) cores into the LMP. As shown in Figure 5b, the EPR shows a featureless single peak with an extremely broad spectral band width. Neither the narrow Dysonian peak shape of conducting electrons in a reduced layer nor an axial signal of a Mo_2(II,III) core[59b] is observed. Although line broadening in EPR spectra is observed for inhomogeneous spin systems, the extreme breadth of the spectral line width (~750 G peak-to-peak separation) in Figure 5b suggests that magnetic ordering resulting from strong spin–spin interactions is an important contributing factor to the broad line width.[89] Similar to the Na^+ intercalate, deviations

(80) Barklie, R. C.; Girard, O.; Braddel, O. *J. Phys. Chem.* **1988**, *92*, 1371.
(81) Kadish, K. R.; Maija, B. G.; Araullo-McAdams, C. *J. Phys. Chem.* **1991**, *95*, 427.
(82) Tachez, M.; Theobald, F.; Bordes, E. *J. Solid State Chem.* **1981**, *40*, 280.
(83) (a) Feher, G.; Kip, A. F. *Phys. Rev.* **1955**, *98*, 337. (b) Feher, G.; Kip, A. F. *Phys. Rev.* **1954**, *95*, 1343.
(84) Wertz, J. E.; Bolton, J. R. *Electron Spin Resonance: Elementary Theory and Practical Applications*; McGraw-Hill: New York, 1972.
(85) Beltran-Porter, D.; Amoros, P.; Ibanez, R.; Martinez, E.; Beltran-Porter, A.; Le Bail, A.; Ferey, G.; Villeneuve, G. *Solid State Ionics* **1989**, *32/33*, 57.
(86) Rushbrooke, G. S.; Wood, P. J. *Mol. Phys.* **1958**, *1*, 257.
(87) Lines, M. E. *J. Phys. Chem. Solids* **1970**, *31*, 101.
(88) Villeneuve, G.; Lezama, L.; Rojo, T. *Mol. Cryst. Liq. Cryst.* **1989**, *176*, 495.

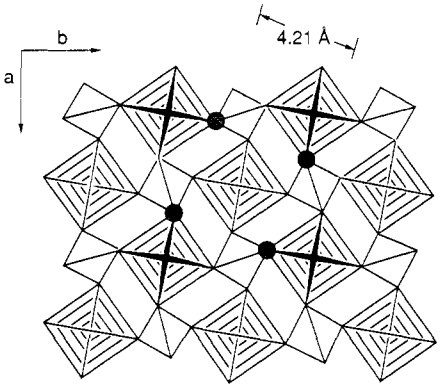

Figure 7. View of the 001 plane of a $VOPO_4 \cdot 2H_2O$ layer. The four oxygens defining a tetragonal cavity in the *a,b*-plane are shown by the shaded circles.

from Curie–Weiss behavior are observed with implications of large antiferromagnetic ordering. The $\chi_M T$ vs T plot shown in Figure 6b reveals antiferromagnetic behavior according to eq 4 with a significant increase in $J/k = -1.75$ K as compared to the Na^+ intercalate. This result shows increased spin interactions within the magnetic layers, thereby suggesting that a spin–spin interaction furnished by nearby paramagnetic Mo_2(II,III) centers may contribute to the broadening in the EPR. An experiment supporting this contention is that the width of the EPR line is reduced to ~100 G upon exposure of the layered intercalate to air (Figure 5c). It is known that the mixed-valence Mo_2(II,III) tetraphosphate core rapidly oxidizes in air to the diamagnetic Mo_2(III,III) triple-bonded species.[60] The observation of line narrowing is consistent with the depletion of the Mo_2(II,III) paramagnet within the layers by oxidation.

Finally it is interesting that the absorption and magnetic spectroscopic studies confirm ESCA and powder X-ray diffraction results inasmuch as a Mo_2(II,III) intercalate is obtained by either Schemes I or II for both the vanadium and niobium phosphates. Our studies on Mo_2(II,II) coordinated by tetraphosphate anion, $Mo_2(HPO_4)_4^{4-}$, show that it is extremely susceptible to oxidation to the mixed-valence $Mo_2(HPO_4)_4^{3-}$ ($E_{1/2}(Mo_2(HPO_4)_4^{3-/4-}) = -0.67$ V vs SCE) dimer.[59b] Indeed, solutions of $Mo_2(HPO_4)_4^{4-}$ are smoothly converted to $Mo_2(HPO_4)_4^{3-}$ by the weakly oxidizing triple-bonded complex $Mo_2(HPO_4)_4^{2-}$ in a simple comproportionation reaction. Presumably, the Mo_2(II,II) core is not stable in a phosphate environment, and parallel to the molecular solution chemistry, the mixed-valence Mo_2(II,III) bimetallic center is the thermodynamic product.

Structural Chemistry. Intercalation of the LMP layers by Na^+ and Mo_2^{5+} ions causes a shift of d_{001} peaks to higher angles thereby signifying a contraction of the LMP gallery height. The placement of negative charges onto the layer with concomitant insertion of positively charged metal ions should enhance the interaction between host layers and guest molecules. To this end the compression of layers about small positively charged cations, as compared to the *d*-spacing of $MOPO_4 \cdot nH_2O$ layers, may be attributed to the electrostatic interaction of the intercalate being much stronger than the hydrogen bonding interactions of the native LMP structure. In support of this contention is a recent EXAFS study regarding the location of guest ions residing in vanadium phosphate galleries.[90] Intercalation of Fe^{3+}, Co^{2+}, and Ni^{2+} also yields layers with contracted *d*-spacings. According to coordination geometries deduced from EXAFS, the most probable location of intercalated metal ions is a tetragonal pocket defined by the four in-plane vanadium octahedra. Within this pocket, four oxygens which are corner-shared between vanadium octahedra and phosphate tetrahedra are available for coordination to guest cations.

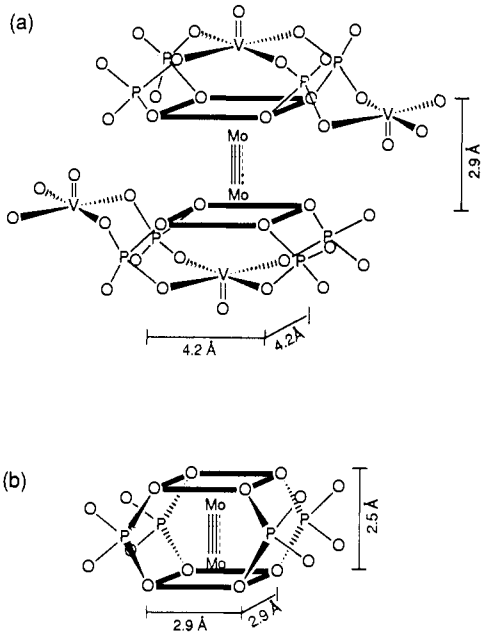

Figure 8. The dimensions of (a) the tetragonal oxygen coordination environment for Mo_2^{5+}-intercalated $VOPO_4$ and (b) the oxygen environment of $Mo_2[O_2P(OC_6H_5)_2]_4(BF_4)$ as determined from the X-ray crystallographic data of ref 59c.

These four oxygens, which are indicated by shaded circles in the *a,b*-plane of the LMP layer shown in Figure 7, are ideally suited for Mo_2^{5+} coordination. Indeed, infrared spectra show no appreciable change in the vanadyl stretch upon intercalation of the Mo_2^{5+} core (<3 cm^{-1}), whereas a ~10-cm^{-1} shift to lower energy is observed for the d(O–P–O) vibration at 400 cm^{-1}. This small shift in the phosphate spectral region suggests a weak guest–host interaction between the Mo_2^{5+} core and oxygens of the phosphate layer. The *d*-spacing of the Mo_2^{5+}-intercalated LMP is also consistent with the binuclear core keying into the tetragonal oxygen cavities of the layer. By using the crystallographic data of Tietze,[91] a layer thickness of 3.6 Å is calculated for the LMP; and on the basis of the observed 6.45-Å *d*-spacing, we determine the intergallery height of the Mo_2^{5+} intercalate to be 2.8 Å. The dimensions of the tetragonal cavity defined by these eight oxygens in neighboring interlayers are summarized in Figure 8a. This configuration of oxygens defines a coordination environment well-suited for the transverse disposition of the Mo_2^{5+} core between LMP interlayers. In this arrangement, four oxygens from each layer provide the coordination sphere for one molybdenum center of the bimetallic core. This "solid state" coordination environment of the intercalated Mo_2^{5+} core is congruent with the molecular crystal structure of the mixed-valence diphenyl phosphate, $Mo_2[O_2P(OC_6H_5)_2]_4(BF_4)$,[59c] and more generally multiply bonded "Mo_2O_8" coordination spheres.[92-94] In these species, a tetragonal cavity is formed from each oxygen of a bridging ligand; the dimensions of the cavity deduced from the X-ray crystal structure of $Mo_2[O_2P(OC_6H_5)_2]_4^+$ are summarized in Figure 8b. The distance of 2.5 Å between oxygen planes for the molecular species is consistent with the observed *d*-spacing of the Mo_2^{5+} intercalate. Alternatively, a similar tetragonal arrangement of oxygens about the Mo_2^{5+} core cannot be achieved when the metal–metal axis is parallel to the host layers. The 4.12-Å distance between intraplanar oxygens (see Figure 7) is too long to sustain the metal–metal interaction of typical mixed-valence dimolybdenum cores. Moreover, we calculate a gallery height of

(89) Bencini, A.; Gattechi, D. *EPR of Exchange Coupled Systems*: Springer-Verlag: New York, 1990.
(90) Antonio, M. R.; Barbour, R. L.; Blum, P. R. *Inorg. Chem.* **1987**, *26*, 1235.
(91) Tietze, H. R. *Aust. J. Chem.* **1981**, *34*, 2035.
(92) Cotton, F. A.; Walton, R. A. *Multiple Bonds Between Metal Atoms*; Wiley-Interscience: New York, 1982.
(93) Robbins, G. A.; Martin, D. S. *Inorg. Chem.* **1984**, *23*, 2086.
(94) (a) Cotton, F. A.; Norman, J. G.; Stults, B. R.; Webb, T. R. *J. Coord. Chem.* **1976**, *5*, 217. (b) Cotton, F. A.; Frenz, B. A.; Pedersen, E.; Webb, T. R. *Inorg. Chem.* **1975**, *14*, 391. (c) Cotton, F. A.; Frenz, B. A.; Webb, T. R. *J. Am. Chem. Soc.* **1973**, *95*, 4431.

4.5 Å (d_{001}(calc) = 8.12 Å) for the parallel disposition of the binuclear core in the layers, which is 1.7 Å greater than the observed *d*-spacing.

A transverse arrangement of the Mo_2^{5+} core permits interlayer keying of the host with the guest structure. This guest-host interaction, which has been observed by us previously in the ion-exchange chemistry of *trans*-dioxorhenium(V) complexes in layered oxides,[47] may provide a clue to the anomalous magnetic behavior of the Mo_2^{5+} intercalate. The observed enhancement in spin-spin coupling may result from increased interlayer communication owing to the smaller *d*-spacing of the Mo_2^{5+} intercalate (d_{001} = 6.4 Å) as compared to the Na^+-intercalated (d_{001} = 6.7 Å) species. However, the EPR experiments show that the spin interactions within the layers are obviously modulated by the physical linkage of a magnetically active $S = {}^1/_2$ guest. The arrangement of spin $^1/_2$ guests keyed into the two-dimensional magnetic layer should give rise to an anisotropic magnetic exchange interaction, thereby modifying the magnetic behavior of the layers. Indeed, the observance of unusual magnetism upon the synthesis of two-dimensional magnetic host layers intercalated with a magnetic guest has precedent. Clement et al. have described spontaneous magnetization below ~90 K for layered $FePS_3$ intercalated with pyridinium.[95] Our results coupled with those of Clement suggest that the ability to synthesize lamellar solids with anisotropically arranged magnetic guests may lead to interesting magnetically-ordered systems.

Thus layered metal phosphate are ideal host structures for M$\overset{4}{-}$M guests. The physical and chemical properties of LMPs are compatible with those properties of M$\overset{4}{-}$M cores, and indeed the coordination environments of M$\overset{4}{-}$M centers in molecular solids can be achieved within the gallery regions of LMPs. In the context of designing photoactive M$\overset{4}{-}$M—LMP intercalates, investigations of tetrakis(phosphato)dimolybdenum have shown their photoredox chemistry to be restricted to one-electron transformations owing to the inability of the rigid phosphate coordination sphere to stabilize high oxidation states of the metal core.[46] Conversely, multielectron phototransformations are promoted at M$\overset{4}{-}$M cores when coordinated by ligands that can stabilize metals in high formal oxidation states. One such class of complexes is the $M_2X_4(\overline{LL})_2$ species, where $\overline{LL}$ is a bidentate phosphine or hydroxypyridine. Upon excitation, rearrangement of the halide ligands to yield bioctahedral geometries promotes the two-electron photooxidations of these M$\overset{4}{-}$M species.[46] To this end, studies are underway to introduce M$\overset{4}{-}$M cores into LMP galleries that are modified with $\overline{LL}$ functionality.

Acknowledgment. We thank Matt Espe for assistance in obtaining low-temperature EPR. Financial support from the National Science Foundation (CHE-9100532) and the Center for Fundamental Materials Research is gratefully acknowledged.

Supplementary Material Available: A table listing the observed and calculated peak positions and the indices of powder X-ray diffraction patterns of layered metal phosphates, ESCA spectra of $NbOPO_4 \cdot 3H_2O$, Na^+-intercalated $NbOPO_4$ host layers and of the solids obtained from the reaction of $[Mo_2(CH_3CN)_8](BF_4)_4$ with $NbOPO_4 \cdot 3H_2O$ and Na^+-intercalated $NbOPO_4$, and powder X-ray diffraction patterns of $NbOPO_4 \cdot 3H_2O$, Na^+-intercalated $VOPO_4$ host layers and of the solids obtained from the reaction of $[Mo_2(CH_3CN)_8](BF_4)_4$ with $NbOPO_4 \cdot 3H_2O$ and Na^+-intercalated $NbOPO_4$ (4 pages). Ordering information is given on any current masthead page.

(95) Clement, R.; Lomas, L.; Audiere, J. P. *Chem. Mater.* **1990**, *2*, 641.

Generation of Au^{2+} Ions in the Solid State or in Fluorosulfuric Acid Solution and Their Identification by ESR

F. G. Herring,* G. Hwang, K. C. Lee, F. Mistry, P. S. Phillips, H. Willner,† and F. Aubke*

Contribution from the Department of Chemistry, The University of British Columbia, 2036 Main Mall, Vancouver, British Columbia, Canada V6T 1Y6. *Received June 14, 1991*

Abstract: The partial pyrolysis of gold(III) fluorosulfate, $Au(SO_3F)_3$, at temperatures below 145 °C allows the generation of Au^{2+} defects in the solid residue by reductive elimination of $SO_3F^\bullet$ radicals. Solvated Au^{2+} is obtained by the reduction of $Au(SO_3F)_3$ in HSO_3F solution by gold powder at 65 °C. Both systems are studied by ESR and identical high g_{iso} values of g = 2.360 are found. Hyperfine splitting due to ^{197}Au, $I = 3/2$, is observed in frozen solutions of Au^{2+}(solv). Pyrolysis of $Br_3[Au(SO_3F)_4]$ also gives partly pyrolyzed $Au(SO_3F)_3$, with a sufficiently high Au^{2+} ion concentration, to allow a magnetic susceptibility study between 100 and 295 K.

Introduction

Compounds or complexes with gold in the oxidation state +2 are rather uncommon.[1,2] Previously reported examples of isolated compounds may be grouped into three general categories.

(a) *Polynuclear* Au(I)/Au(III) compounds comprise the first category, with gold(II) chloride, Au_4Cl_8,[3] a typical example. As expected, gold(I) exhibits linear, and gold(III) square-planar coordination. The existence of this group, termed "pseudogold(II)" compounds,[2] reflects the tendency of gold(II), $5d^9$, to disproportionate completely into gold(I), $5d^{10}$, and gold(III), $5d^8$.

† Permanent address: Institut für Anorganische Chemie, der Universität, Callinstrasse 9, D Hannover.

(1) (a) Puddephatt, R. J. *The Chemistry of Gold*; Elsevier: Amsterdam, The Netherlands, 1978. (b) Puddephatt, R. J. In *Comprehensive Coordination Chemistry*; Wilkinson, G., Ed.; Pergamon Press: Oxford, U.K., 1987; Vol. 7, p 861.

(2) Schmidbaur, H.; Dash, K. C. *Adv. Inorg. Chem. Radiochem.* **1982**, *25*, 39.

(3) (a) Dell'Amico, D. B.; Calderazzo, F.; Marchetti, F.; Merlino, S.; Perego, G. *J. Chem. Soc., Chem. Commun.* **1977**, 31. (b) Dell'Amico, D. B.; Calderazzo, F.; Marchetti, F.; Merlino, S. *J. Chem. Soc. Dalton Trans.* **1982**, 2257.

0002-7863/92/1514-1271$03.00/0